

Dynamical Scaling of the Quantum Hall Plateau Transition

F. Hohls,^{1,*} U. Zeitler,¹ R. J. Haug,¹ R. Meisels,² K. Dybko,^{2,3} and F. Kuchar²

¹*Institut für Festkörperphysik, Universität Hannover, Appelstrasse 2, 30167 Hannover, Germany*

²*Department of Physics, University of Leoben, Franz Josef Strasse 18, 8700 Leoben, Austria*

³*Institute of Physics, Polish Academy of Science, Al. Lotnikow 32/46, 02-668 Warsaw, Poland*

(Received 17 July 2002; published 13 December 2002)

Using different experimental techniques, we examine the dynamical scaling of the quantum Hall plateau transition in a frequency range $f = 0.1\text{--}55$ GHz. We present a scheme that allows for a simultaneous scaling analysis of these experiments and all other data in literature. We observe a universal scaling function with an exponent $\kappa = 0.5 \pm 0.1$, yielding a dynamical exponent $z = 0.9 \pm 0.2$.

DOI: 10.1103/PhysRevLett.89.276801

PACS numbers: 73.43.Nq, 64.60.Ht, 73.43.Fj

Phase transitions between different phases of matter are frequently met in nature, e.g., in ice/water, para/ferromagnet, and normal/superconductor. The usual classification distinguishes between first- and second-order transitions. In a first-order transition, the two phases coexist; in a second-order transition, they do not. Such transitions are termed “classical” and occur at nonzero temperature. Different from these types of classical phase transitions are quantum phase transitions. Strictly speaking, they occur only at zero temperature [1]. However, as long as the quantum fluctuations governing the transition dominate the thermal fluctuations, we also can observe them at $T > 0$.

Second-order quantum phase transitions occur at a critical value of a parameter which can be, e.g., the disorder in the metal-insulator transition of two-dimensional electron systems at zero magnetic field or the magnetic field in the transition between quantum Hall (QH) plateaus in such systems [2,3]. The latter one is the target of the investigations presented in this Letter.

Generally, when the transition is approached, the correlation length ξ of the quantum fluctuations diverges in form of a power law $\xi \propto |\delta|^{-\gamma}$ with γ being the critical exponent. For a QH system δ is the distance from a critical energy E_c which can be identified as the center of a disorder-broadened Landau level. The correlation length corresponds to the localization length $\xi(E)$, which expresses the typical extensions of the wave function at energy E , diverges at E_c :

$$\xi(E) \propto |E - E_c|^{-\gamma}. \quad (1)$$

For an infinitely large sample at $T = 0$ K, the quantum phase transition from one quantum Hall state at $E < E_c$ to another one at $E > E_c$ happens via a single metallic (extended) state at the critical point E_c ; all other states are localized. In contrast, in a finite sample the states with a localization length larger than the sample size L are effectively delocalized; the transition is smoothed onto a finite energy range. Additionally, at nonzero tempera-

ture and nonzero measuring frequency further sources of effective delocalization come into play.

The finite size dependence of the wave functions was investigated in a number of numerical calculations [4–6] for noninteracting electrons. They confirmed localization length scaling [Eq. (1)] in quantum Hall systems with a universal scaling exponent $\gamma = 2.35 \pm 0.03$, independent of the disorder potential [2]. Short-range interactions are predicted not to change the critical exponent [7]. However, the effect of long-range electron-electron interaction present in the experiments remained unclear.

Experimentally, neither the wave function nor the energy E are directly accessible. Instead, we measure the conductivity $\sigma_{xx}(B)$ as a function of the magnetic field B , observing quasimetallic behavior ($\sigma_{xx} \sim e^2/h$) near some critical field B_c , where the state at the Fermi energy is extended [$\xi(B) > L$], and insulating behavior ($\sigma_{xx} \ll e^2/h$) for localized states [$\xi(B) \ll L$]. More generally, theory predicts the conductivity to follow general functions [8] $\sigma_{ij}(B) = G(L/\xi) = G_L(L^{1/\gamma}\delta B)$, where we have used Eq. (1) and linearized $\delta B = B - B_c \propto E_c - E$ near the critical point. Then the width of the quasimetallic region ΔB , called plateau transition width, follows $\Delta B \propto L^{-1/\gamma}$. Such a prediction was indeed verified experimentally [9], yielding $\gamma = 2.3 \pm 0.2$. Quite recently, this value was also confirmed by indirect measurements of the localization length $\xi(B)$ in the “insulating” variable range hopping regime [10,11].

Nonzero temperature $T > 0$ or frequency $f > 0$ introduce additional time scales $\tau_T \sim \hbar/k_B T$ or $\tau_f \sim 1/f$ [3]. This time has to be compared to the correlation time $\tau_\xi \propto \xi^z$ with a dynamical exponent z . In a more descriptive approach, the additional time scale τ can be translated into an effective system size $L_{\text{eff}} \propto \tau^{1/z}$. Plugging this into $\sigma_{ij} = G_L(L^{1/\gamma}\delta B)$, we find scaling functions

$$\begin{aligned} \sigma_{ij}(f, T = 0) &= G_f(f^\kappa \delta B) \quad \text{and} \\ \sigma_{ij}(f = 0, T) &= G_T(T^\kappa \delta B) \end{aligned} \quad (2)$$

with a universal scaling exponent $\kappa = 1/z\gamma$. The

transition widths are then given by $\Delta B \propto T^\kappa$ and $\Delta B \propto f^\kappa$. When identifying τ with the phase coherence time, L_{eff} is interpreted as the phase coherence length and given by diffusion: $L_{\text{eff}}^2 \sim D\tau$. This yields a dynamical exponent $z = 2$ validated in a numerical calculation of the frequency dependence of σ_{xx} for noninteracting electrons [12]. While z is not affected by short-range interactions [13], it has been claimed that long-range Coulomb interaction changes the dynamical exponent to $z = 1$ [14,15].

Temperature scaling experiments done so far yield an ambiguous picture. While first experiments on InGaAs quantum wells claimed to observe scaling with a universal exponent $\kappa = 0.42 \pm 0.04$ [16], a number of other experiments reported either scaling with a sample dependent κ [17] or even doubted the validity of scaling at all [18]. For frequency scaling, the evidence is even worse. Engel *et al.* [19,20] claim to observe scaling for two different samples with $\kappa \approx 0.42$; an experiment of Balaban *et al.* [21] contradicts scaling. In addition, all of these experiments did not obey $hf \gg k_B T$ and, therefore, any single-parameter scaling analysis cannot be straightforwardly applied.

To overcome these limitations, we combine in this work experiments covering a frequency range 0.1–55 GHz. We have measured the conductivity σ_{xx} in two different setups. Our results are complemented with data from literature [19–22]. Using all these data [10,19–25], we demonstrate a universal function with a universal scaling exponent $\kappa = 1/z\gamma = 0.5 \pm 0.1$, yielding a dynamical scaling exponent $z = 0.9 \pm 0.2$.

Up to 6 GHz the sample conductivity is measured in a coaxial reflections setup as described in detail in Refs. [10,23]. The sample, patterned into Corbino geometry, acts as a load of a coaxial cable fitted into a $^3\text{He}/^4\text{He}$ dilution refrigerator. The two-dimensional electron system (2DES) used in these experiments was realized in an AlGaAs/GaAs heterostructure with electron density $n_e = 3.3 \times 10^{15} \text{ m}^{-2}$ and mobility $\mu_e = 35 \text{ m}^2/\text{V s}$. Traces of $\sigma_{xx}(B)$ shown in Fig. 1(a) reveal a peak at every transition between QH states. The spin-split transitions are resolved up to a filling factor $\nu = n_e h/eB = 6$. The transition widths ΔB measured as the full width at half maximum of the peaks are shown in Fig. 1(c) [26]. For $f \leq 1$ GHz, ΔB is governed by the temperature $T \approx 0.1$ K of the 2DES as deduced from temperature dependent measurements at $f = 0.2$ GHz. Above 2 GHz frequency scaling $\Delta B \propto f^\kappa$ takes over.

In a second experiment, we use waveguides to access frequencies from 26 to 55 GHz. The AlGaAs/GaAs heterostructure is placed at the end of the waveguide and partially reflects the incident microwave. To eliminate artifacts not originating from the 2DES, e.g., due to a change of the index of refraction at the sample surface, we modulate the carrier density using a thin front gate 70 nm above the 2DES. The high sheet resistance $R \approx 2k\Omega/\square$ of the gate is about 4 times larger than

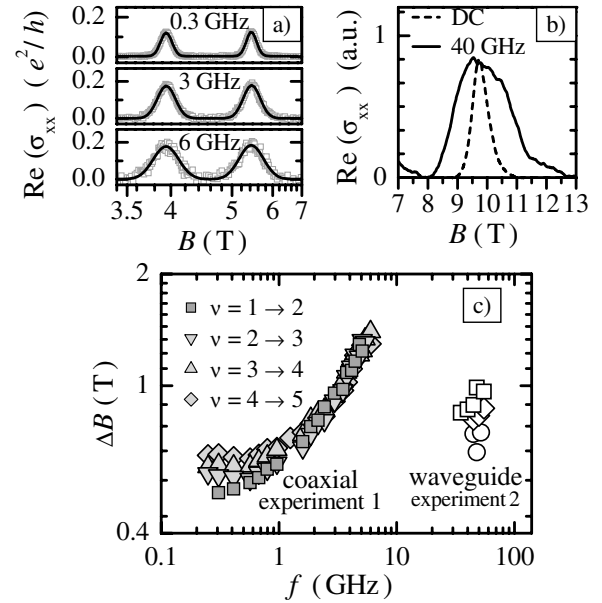


FIG. 1. (a) Conductivity of sample 1 measured in the coaxial setup. Here shown are the conductivity peaks at the $\nu = 4 \rightarrow 3$ and $\nu = 3 \rightarrow 2$ plateau transition. (b) Conductivity of sample 2 at the $\nu = 2 \rightarrow 1$ transition, measured in the waveguide reflection setup for very high frequencies and in a classical Hall setup for dc. (c) Frequency dependence of the width of the QH plateau transitions, measured for $\nu > 2$ as full width and for $\nu = 2 \rightarrow 1$ as half width at half maximum [24,26]. For the waveguide experiment, different symbols denote different samples from the same wafer or different cooldown cycles with slightly different carrier densities.

the waveguide impedance and allows a sufficient transmission of the microwave field. For details of the setup, see [24,25]. The electron density and mobility of the 2DES are $n_e = 3.6 \times 10^{15} \text{ m}^{-2}$ and $\mu_e = 10 \text{ m}^2/\text{V s}$. The use of a low mobility sample ensures that hf (0.2 meV at 50 GHz) is smaller than the Landau level width (~ 1 meV). For higher Landau levels we do not observe a distinct spin splitting and thus concentrate for this experiment on the width of the $\nu = 1 \rightarrow 2$ transition. This limitation also ensures that the cyclotron frequency $f_c \approx 4$ THz is much larger than the measurement frequencies $f \leq 55$ GHz. The measured conductivity $\sigma_{xx}(B)$ at a temperature of $T = 0.3$ K is shown in Fig. 1(b); the evaluated transition widths [26] are depicted in Fig. 1(c).

The combination of our two experimental techniques allows us to investigate the scaling behavior of the QH plateau transition in a large frequency range. Additionally, we can compare our results to all other frequency scaling experiments. Table I summarizes the wide ranges of the parameters such as frequency, mobility, density, temperature, filling factor, and material, which were covered by the different experiments [10,19–25]. The observed frequency dependencies of the transition width ΔB are summarized in Fig. 2.

TABLE I. Key data of the compared experiments: 2DES mobility μ_e in m^2/Vs , analyzed range of filling factor ν , 2DES temperature T , and frequencies f . The heterostructures used were InGaAs/InP in Ref. [20] and AlGaAs/GaAs otherwise.

Experiment	μ_e	ν	T (K)	f (GHz)
Coax.[10,23]	35	1–5	0.1	0.1–6
Waveg. [24,25]	10	1–2	0.3	35–55
Engel [19]	4	1–2	0.14–0.5	0.2–14
Shahar [20]	3	0–1	0.2–0.43	0.2–14
Balaban [21]	3	1–2	0.15	0.7–7
Lewis [22]	50	3–5	0.24–0.5	1–10

Since most of these data do not fulfill $hf \gg k_B T$, we have to take into account the influence of both frequency f and temperature T for our analysis. Therefore, the single-parameter scaling functions for the plateau transition [Eq. (2)] are modified using a two-variable scaling analysis $\sigma_{ij}(T, f) = G_{T,f}(T^\kappa \delta B, f^\kappa \delta B)$ [3], p. 327.

Both hf and $k_B T$ set an energy scale. Since frequency and temperature act as independent processes, it is a reasonable ansatz to sum the energies squared [28], resulting in a combined energy scale $\Gamma = [(\alpha hf)^2 + (k_B T)^2]^{1/2}$. The factor α is of the order of unity and covers the differences of the effects of frequency and temperature. Using this simple model, the transition width scales as $\Delta B \propto \Gamma^\kappa$ and can be rewritten as

$$\Delta B_s(T, f) = \Delta B_s(T) \left(\sqrt{1 + \left(\frac{\alpha hf}{k_B T} \right)^2} \right)^\kappa, \quad (3)$$

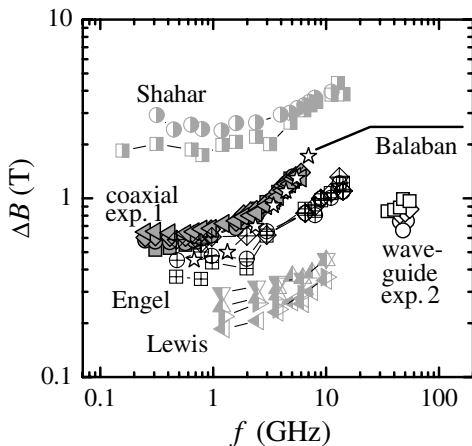


FIG. 2. Comparison of the transition width vs frequency for all experiments [10,19–25]. Multiple symbols for the same experiment denote different samples or cooldowns (waveguide), transitions (coaxial, Lewis), or temperatures (Engel, Lewis, Shahar) as presented in Table I.

with a prefactor $\Delta B_s(T)$ depending only on temperature and on the individual sample s .

We use this equation to combine all data presented in Fig. 2 in a single graph as shown in Fig. 3(a). All the widths $\Delta B(T, f)$ measured in the different experiments are normalized to the dc width $\Delta B(T, f \approx 0)$ and plotted versus the ratio $x = hf/k_B T$ [29]. The lowest 2DES temperature is estimated in the following way: Most authors state the exponent for the temperature dependence of $\Delta B(T)$. Combined with the low-frequency width ΔB at high temperatures where the 2DES still couples thermally to the liquid $^3\text{He}/^4\text{He}$ bath, we extract the lowest 2DES temperature from the $f \rightarrow 0$ saturation width.

All data except those of Ref. [21] fall on a common curve obeying Eq (3), independent of material, mobility, density, experimental technique, temperature, and filling factor, including the quantum Hall to insulator transition analyzed in Ref. [20]. The single deviation observed in Ref. [21], accompanied by deviations from temperature scaling, is probably caused by macroscopic inhomogeneities spoiling universal scaling [30]. We therefore exclude this data from the following scaling analysis.

The observation of a universal curve in Fig. 3 clearly reveals the universality of the quantum phase transition between different Hall plateaus and into the Hall insulator. Although the large scattering of the data does not allow us to exclude a linear dependence $\Delta B = a \times f + b$ proposed in Ref. [21], we find the scaling ansatz

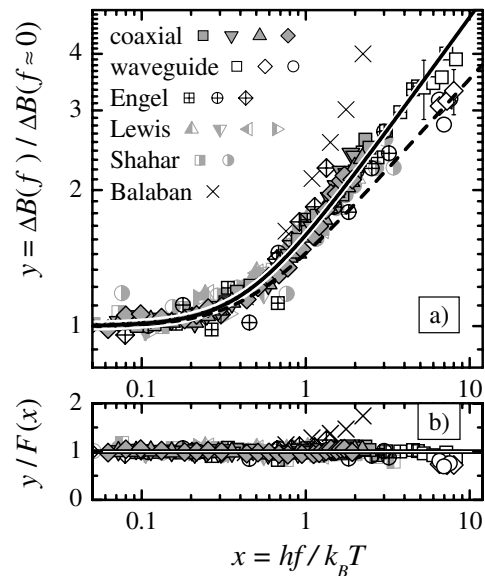


FIG. 3. (a) Normalized plateau transition width $y = \Delta B(f, T)/\Delta B(f \approx 0, T)$ vs $x = hf/k_B T$ for all data presented in Table I and Fig. 2. The solid line results from a fit of $F(x) = [1 + (\alpha x)^2]^{\kappa/2}$ [Eq. (3)] to all data except those for $f > 20$ GHz and the Balaban experiment ($\alpha \approx 2$, $\kappa = 0.5 \pm 0.1$). The dashed line depicts a reduced $\kappa = 0.4$. (b) Rescaling of $y = \Delta B(f, T)/\Delta B(f \approx 0, T)$ by the scaling function $F(x)$ allows one to judge the quality of scaling.

$F(x) = [1 + (\alpha x)^2]^{\kappa/2}$ for this universal curve to be favored by a better result of the statistical χ^2 test. Therefore, it seems reasonable to fit the data to Eq. (3) and to determine the associated universal scaling exponent κ . Such a fit, omitting only the highest frequencies $f > 15$ GHz from the waveguide experiment, which will be treated separately, is shown as a solid curve in Fig. 3 and yields $\alpha \approx 2$ and a scaling exponent $\kappa = 0.5 \pm 0.1$.

Within their individual 2σ error, the data from the waveguide experiment also agree with the fit function $F(x)$, whereas the extrapolation of the linear fit of the low-frequency data would be less favorable. But also for the more suitable scaling function $F(x)$ Fig. 3 reveals that the combined statistical weight of the waveguide data indicates a slightly lower scaling exponent κ between 0.5 and 0.4. This reduction of κ towards its lower limit $\kappa = 0.2$ for a noninteracting 2DES [2,13] possibly hints to a partial screening of Coulomb interaction of the electrons, caused by the gate on top of the sample. The screening is weak due to the large distance of the gate (70 nm) compared to the average electron-electron distance (17 nm). But we might expect a moderate change of the scaling exponent κ as it is predicted to depend mainly on long-range interaction [13].

Having determined the universal scaling exponent $\kappa = 1/z\gamma = 0.5 \pm 0.1$ of the frequency and temperature scaling, we would like to separate the dynamical exponent z and the critical exponent γ . Recent experiments exploited the frequency [10] and the temperature dependence [11] of the conductivity in the variable range hopping regime, which allowed one to determine the localization length $\xi(B)$. Both observed a scaling behavior $\xi \propto |\delta\nu|^{-\gamma}$ with a universal critical exponent $\gamma = 2.3 \pm 0.2$ in agreement with earlier size scaling experiments [9] and astoundingly with the value obtained in numerical studies for noninteracting electrons [4–6]. With this universal scaling exponent $\gamma \approx 2.3$, we can deduce a dynamical exponent $z = 1/\gamma\kappa = 0.9 \pm 0.2$ in agreement with theoretical predictions [14,15].

In conclusion, we have developed a method to combine data from all experiments on frequency scaling of the quantum Hall plateau transition. We find a universal behavior independent of material, density, mobility, experimental technique, temperature, and filling factor, which clearly demonstrates the universal nature of this quantum phase transition. Applying a scaling analysis, we determine the universal scaling exponent of an interacting QH system to $\kappa = 0.5 \pm 0.1$ and, using the critical exponent $\gamma \approx 2.3$, the dynamical exponent to $z = 0.9 \pm 0.2$.

We thank F. Evers, B. Huckestein, B. Kramer, D. G. Polyakov, and L. Schweitzer for useful discussions and R. M. Lewis for providing us with data from his Ph.D.

thesis. This work was supported by the DFG, DIP, and the European Union, Grant No. FMRX-CT98-180.

*Electronic address: hohls@nano.uni-hannover.de

- [1] S. Sachdev, *Quantum Phase Transitions* (Cambridge University, Cambridge, 1999).
- [2] B. Huckestein, *Rev. Mod. Phys.* **67**, 357 (1995).
- [3] S. L. Sondhi *et al.*, *Rev. Mod. Phys.* **69**, 315 (1997).
- [4] H. Aoki and T. Ando, *Phys. Rev. Lett.* **54**, 831 (1985).
- [5] J. T. Chalker and G. J. Danielli, *Phys. Rev. Lett.* **61**, 593 (1988).
- [6] B. Huckestein and B. Kramer, *Phys. Rev. Lett.* **64**, 1437 (1990).
- [7] D.-H. Lee and Z. Wang, *Phys. Rev. Lett.* **76**, 4014 (1996).
- [8] A. M. M. P. Pruisken, *Phys. Rev. Lett.* **61**, 1297 (1988).
- [9] S. Koch *et al.*, *Phys. Rev. Lett.* **67**, 883 (1991).
- [10] F. Hohls, U. Zeitler, and R. J. Haug, *Phys. Rev. Lett.* **86**, 5124 (2001).
- [11] F. Hohls, U. Zeitler, and R. J. Haug, *Phys. Rev. Lett.* **88**, 036802 (2002).
- [12] A. Bäker and L. Schweitzer, *Ann. Phys. (Leipzig)* **8**, SI-21 (1999).
- [13] Z. Wang *et al.*, *Phys. Rev. B* **61**, 8326 (2000).
- [14] B. Huckestein and M. Backhaus, *Phys. Rev. Lett.* **82**, 5100 (1999).
- [15] D. G. Polyakov and B. I. Shklovskii, *Phys. Rev. B* **48**, 11167 (1993).
- [16] H. P. Wei *et al.*, *Phys. Rev. Lett.* **61**, 1294 (1988).
- [17] S. Koch *et al.*, *Phys. Rev. B* **43**, 6828 (1991).
- [18] D. Shahar *et al.*, *Solid State Commun.* **107**, 19 (1998).
- [19] L. W. Engel *et al.*, *Phys. Rev. Lett.* **71**, 2638 (1993).
- [20] D. Shahar, L. W. Engel, and D. C. Tsui, in *Proceedings of the 11th International Conference on High Magnetic Fields in the Physics of Semiconductors*, edited by D. Heiman (World Scientific, Singapore, 1995), p. 256.
- [21] N. Q. Balaban, U. Meirav, and I. Bar-Joseph, *Phys. Rev. Lett.* **81**, 4967 (1998).
- [22] R. L. Lewis, Ph.D. thesis, Indiana University, Bloomington, 2001.
- [23] F. Hohls *et al.*, *Physica (Amsterdam)* **298B**, 88 (2001).
- [24] K. Dybko *et al.*, in *Proceedings of the 25th International Conference on Physics of Semiconductors*, edited by N. Miura and T. Ando (Springer, Berlin, 2001), p. 915.
- [25] F. Kuchar *et al.*, *Europhys. Lett.* **49**, 480 (2000).
- [26] Due to an impurity related shoulder appearing on the low filling side [27], we only use the high filling side of this transition for determining ΔB . The critical point B_c was fixed at its dc value [24].
- [27] R. J. Haug *et al.*, *Phys. Rev. Lett.* **59**, 1349 (1987).
- [28] Simply adding the energies ($\Gamma = k_B T + ahf$) does not fit our data.
- [29] L. W. Engel, Y. P. Li, and D. C. Tsui, *Physica (Amsterdam)* **227B**, 173 (1996).
- [30] I. M. Ruzin, N. R. Cooper, and B. I. Halperin, *Phys. Rev. B* **53**, 1558 (1996).